Linear and Nonlinear Properties of Graphene at Millimeter-Wave for Multiplier and Mixer Applications

Amr Samir[1], Hesham El-Sherif[2], Sherif Kishk[1],
Maher AbdelRazzak[1], and Mohamed Basha[3, *]

Abstract—In this paper linear and nonlinear properties of graphene at millimeter wave frequency band are investigated. The nonlinear properties of the graphene are utilized to design frequency multiplier and mixer for millimeter wave applications. A patch of graphene is deposited on the dielectric image guide that will generate higher order harmonics. The amplitude of harmonics is optimized based on the dimensions of the graphene patch on top of the dielectric image guide. A frequency multiplier and mixer are designed, which utilize the second harmonics generated through graphene. The nonlinear behavior of the proposed designs has been simulated in the 50–75 GHz input signal frequency range. A conversion efficiency of -23 dB is obtained for the second harmonic for the frequency doubler. The frequency mixer is designed to mix two frequencies in V-band using dielectric image guide as the waveguide. A -28 dB conversion efficiency is simulated on a dielectric image-guide platform.

1. INTRODUCTION

The saturation in the microwave spectrum and the rapid development of nowadays technology have forced most of communications research centers and service providers to search for an alternative at higher frequencies. Millimeter and sub-millimeter wave bands not only offer a convenient solution for the spectrum congestion problem but also give a very high data transmission rate [1–3] and increased security systems [4, 5] which make it vital for many military and civilian applications [6, 7]. There are lots of improvements going on nowadays in using these bands, and they are expected to deprecate most of the currently used systems in the near future. A low cost and high performance receiver in millimeter wave communication systems is the target that every designer challenges to achieve by enhancing its components such as antennas, filters, frequency mixers and even the interconnects of the circuit.

Dielectric waveguides and image guides offer a great solution to transfer electromagnetic energy with very high efficiency at millimeter wave bands due to absence of metallic losses [8, 9]. The present work focuses on implementing nonlinear components on dielectric platforms based on graphene material as the basic nonlinear element.

Graphene as the first example of a 2D material has very extreme electrical and photonic properties, which receives the attention of THz and optical regimes in recent years [10]. One basic parameter of graphene model is its complex conductivity ($\sigma_g = \sigma_{gr} \pm i\sigma_{gi}$) which depends on frequency ω of incident wave, Γ charged particle scattering rate which represents loss mechanism, temperature T, and chemical potential μ_c which depends on the carrier density. Chemical potential is a very important parameter as it can be controlled by static electric field caused by changing gate voltage or by using chemical doping.

The nonlinear behavior of graphene material is very strong and theoretically predicted for single and multi-layers to have odd order harmonic components [10]. This theoretical prediction has been experimentally verified at microwave, millimeter and optical frequency ranges but accompanied by even order harmonics as well. This remarkably strong nonlinear effect was modeled for graphene to have a nonlinear susceptibility of the third order $|\chi(3)| = 10^{-15}\,\mathrm{m}^2/\mathrm{v}^2$ which has efficiency much higher than any other nonlinear semiconductor materials [11–13].

At millimeter and sub-terahertz wave ranges, the fabrication of frequency conversion devices such as multipliers and mixers is very complex and expensive, specially for high multiplication orders. Currently existing solid state technologies like Schottky barrier diodes and Hot-electron bolometer [14–16] achieve high frequency conversion efficiency for the second and third orders. However, for higher order harmonics the power tends to decay rapidly for a single stage device.

Section 2 provides a brief description of the band structure for graphene material and its electronic model parameters such as surface conductivity and effective dielectric constant, and Section 3 is a full transfer and characterization of graphene sheet to ensure its quality measurement, its surface resistivity, transmission and number of graphene layers with existing impurities using Raman's spectroscopy. In Section 4, a frequency multiplication device is designed based on graphene material's nonlinearity on dielectric image guide and simulated to calculate its conversion efficiency, and in Section 5, a graphene based frequency mixer design is proposed, and verified results in simulation are shown in Section 6.

2. MODEL OF GRAPHENE

Graphene is a two-dimensional single atomic planar sheet of sp^2 bonded carbon atoms that are densely packaged into a honeycomb lattice structure. Graphene has a very special band structure as the two bands meet at one point called Dirac Point, and the Energy Momentum curve is linear (not parabolic as most materials). This structure of graphene leads to extraordinary electronic properties like its superconductivity and nonlinear behavior. In ideal situation, zero temperature and no doping, the Fermi level is at Dirac point so the lower band is occupied, and the upper band is empty. Near this Dirac point, the electrons act as massless particles with linear dispersion, and this unique behavior anticipates a strong nonlinear response which produces intense high order harmonics with significantly high conversion efficiency.

Graphene is usually characterized using a surface conductivity rather than a volumetric permittivity. In this work, permittivity has been estimated using the surface conductivity model of graphene material [17]. The surface conductivity for a single layer of graphene is given by

$$\sigma_{Graphene}\left(\omega, \Gamma, \mu_c, T\right) = \sigma_{intra}\left(\omega, \Gamma, \mu_c, T\right) + + \left(\omega, \Gamma, \mu_c, T\right) \tag{1}$$

where ω is the radian frequency, μ_c the chemical potential, Γ the phenomenological scattering rate, and T the temperature. Introducing a graphene layer into a simulation requires a conversion of the surface conductivity into a volumetric anisotropic permittivity. A graphene layer can be modeled using a uniaxial anisotropic permittivity by assuming finite thickness of the graphene layer. The permittivity can be estimated from conductivity model using the following relation,

$$\varepsilon_{Graphene}\left(\omega, \Gamma, \mu_c, T\right) = \varepsilon_r + i\frac{\sigma\left(\omega, \Gamma, \mu_c, T\right)}{\varepsilon_o \omega \Delta} \tag{2}$$

where Δ is the graphene thickness, and hence the volumetric complex permittivity is deduced from Equations (1) and (2) as:

$$\varepsilon_{Graphene}\left(\omega, \Gamma, \mu_c, T\right) = \varepsilon_r - \left(\frac{\mu_c e^2 \omega}{\pi\hbar^2\left(\omega^2 + \tau^{-2}\right)}\right)\frac{1}{\varepsilon_o \omega \Delta} + i\left(\frac{\mu_c e^2}{\pi\hbar^2\left(\omega^2 + \tau^{-2}\right)\tau}\right)\frac{1}{\varepsilon_o \omega \Delta} \tag{3}$$

The nonlinearity of graphene has been studied extensively and verified experimentally to be widely used in many applications including harmonic generation, frequency mixers, optical rectification, amplifiers and many other nonlinear devices [18, 19]. Generally, the nonlinear effect occurs when a material responds in a not linearly proportional way to the interacted incident radiation field. The induced polarization in this case can be represented by a power series in field strength as:

$$P(t) = \epsilon_0 \chi_1 E(t) + \chi_2 E_2(t) + \chi_3 E_3(t) + \ldots \tag{4}$$

Here χ^1 denotes linear susceptibility of the material, and χ^2 and χ^3 denote the second and third order susceptibilities that describe the nonlinear effect in the material. Due to linear dispersion of electrons, response of graphene to an external electromagnetic field turns out to be intrinsically nonlinear. This nonlinear effect can simply be explained by its energy electron velocity relation [20],

$$E_{p2} = Vp = V\sqrt{Px^2 + Py^2} \tag{5}$$

where v and p are electron's velocity and momentum in the two directions of the 2D lattice, respectively, and the induced current on graphene will have higher harmonics for a single time harmonic electric field exposure to the material due to its nonlinear relation between its energy and electron velocity [20].

$$j_x(t) = en_sV\frac{4}{\pi}\left\{\sin\Omega t + \frac{1}{3}\sin 3\Omega t + \frac{1}{5}\sin 5\Omega t + \dots\right\} \tag{6}$$

where j_x is the graphene's surface induced current, e the electron charge, V the electron's velocity, and Ω the angular frequency. This result theoretically predicts odd order harmonics for interaction of electric field with graphene material, and the third order nonlinear susceptibility is estimated in [21] to be $\chi^3 \sim 10^{-7}$ which is 10^5 times higher than that in silicon.

3. GRAPHENE CHARACTERIZATION

3.1. Graphene Transfer on Glass Substrate

A graphene sheet of $1\,\mathrm{cm} \times 1\,\mathrm{cm}$ is on a Cu foil purchased from an external provider [22]. The sheets were manufactured by CVD method above an annealed copper substrate of $18\,\mathrm{\mu m}$ thickness. The top side of the copper substrate was coated by less than $100\,\mathrm{nm}$ Poly-Methyl-Meth-Acrylate (PMMA) layer, as illustrated in Fig. 1. It is worth mentioning that the CVD process produces two graphene layers on top and back sides of the copper substrate where the two copper surfaces were subjected to the carbon deposition during the CVD process inside the tube furnace. However, the top side of graphene layer is the desired one which is coated by a PMMA layer for the transferring purposes.
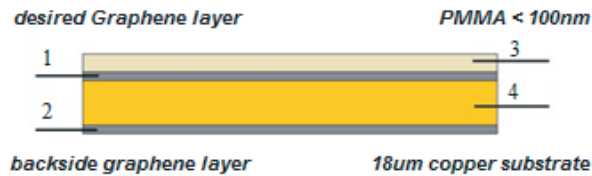
Figure 1. Cross-section drawing of commercial Graphene layer.
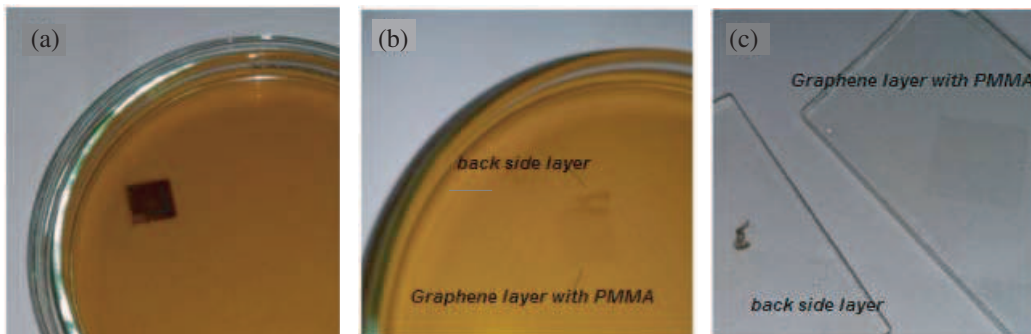
Figure 2. Graphene transferring process, (a) etching copper in ferric chloride solution, (b) after 20 minutes of etching, (c) transferring the graphene layer on glass substrate.

The graphene sheet was transferred from the copper substrate to a glass substrate for characterization by the standard Acetone method. Before transferring, all instruments are cleaned by deionized water and ISO propanol then heated at 70°C for 30 minutes. One mole ferric chloride (FeCl$_3$) solution is prepared for etching the copper layer. A 30 mL of the ferric chloride is placed in a petri dish, then the graphene product is placed carefully on the liquid surface as shown in Fig. 2(a). The copper layer is etched completely after 20 minutes. As illustrated in Fig. 2(b), the graphene layer with the PMMA layer floats on the ferric chloride surface while the back side graphene precipitates away to the bottom of the petri dish. Glass substrates are used to extract the graphene with PMMA and the back side graphene as in Fig. 2(c). The graphene layer with PMMA is cleaned twice in deionized water, then the substrate is dried to 90°C for 20 minutes in order to remove any residual liquid water from the washing process in addition to improve the staking of the graphene layer to the glass substrate. Finally, the graphene with PMMA layer is submerged in 30 mL Acetone for 18 hours at 20°C room temperature in order to remove the PMMA layer.

3.2. Graphene Characterization

The graphene layer over the glass substrate is characterized in order to ensure the quality of the graphene layer and the transferring process. Optical microscope is used to image the graphene edges, and the PMMA residuals at 50 and 500 magnification. Atomic Force microscope attached with the NeaSNOM microscopy system is used to image the surface of graphene wrinkles, PMMA residuals, and defected holes within the sheet. The Gain and Time constants are adapted to make better interaction between the AFM feedback system and the graphene sample. The AFM scans different square areas of 5, 20, and 100 µm lengths. Image analysis is done by Gwyddion software.

Raman spectroscopy was used to characterize the number of graphene layers and the existence of impurities by using red laser with 2.41 eV energy. Spectrophotometer analysis is used to measure the sheet transmission. Finally, a four-point probe (model: Jandel RM3000) was used for measuring the sheet resistance at a constant current supply of 4.5324 µA. The device has 4 Tungsten probes of 400 µm diameter and 12.5 µm end radii. The four probes have 1 mm distance from each other. The four terminals were gently approached on the graphene sheet to make a contact. Different positions of contact were tested within the area of the prepared graphene. The measured data were transferred from the Jandel controller to a PC for storing and processing.

As shown in Fig. 3(a), the graphene sheet is well transferred without crumplings. However, there are residual PMMA particles of average size of 10 µm as illustrated in Figs. 3(b), (c). Image software is used to determine the percentage of residual PMMA in the shown field of Fig. 3(c). Residual PMMA is about 12%.

Due to the thermal expansion difference between graphene and copper substrate during the CVD process, there are wrinkles across the grain boundaries of the copper substrate. There are about 5
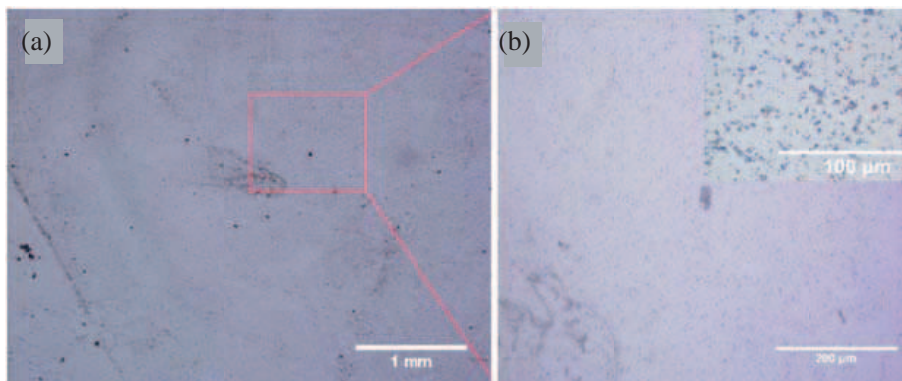
Figure 3. Optical microscope images of transferred graphene sheet after cleaning with acetone, (a) over view of small magnification presents the graphene edge, (b) larger magnification presents the residual of PMMA particles.

wrinkles per 1 μm unit length of the grain boundary. The wrinkles width is about 2 μm, and the average height is 4 nm as illustrated in Fig. 4. It is worth mentioning that the wrinkles increase the overall sheet resistance. So it is aimed to decrease the wrinkles density as much as possible.

The Raman Spectrum in Fig. 5 shows the typical lD, G, and 2D bands of 1319.5, 1575, and 2668 cm^{-1}, respectively. The values of the peaks are close to the literature data [23] with error less than 2.5%. The 2D peak is three times of the G peak which indicates that the sample is monolayer graphene.

The transmission curve in Fig. 6 presents a minimum transmission of 93.9% around 330 nm wave length. This value is different from the literature data which indicate a 270 nm wavelength [24]. This may be due to the existence of PMMA residuals on the graphene sheet. The average transmission in the visible light spectrum is 98.7% which is larger than the literature value (95.2%) in [24].
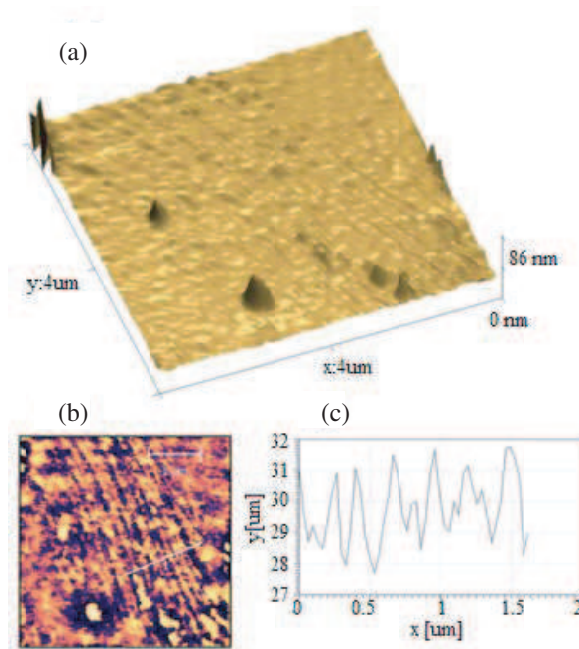
Figure 4. Atomic Force Microscopy of graphene sheet, (a) 3D overview of 4.0×4.0 μm area shows the graphene wrinkles due to the preparation process, (b) 2D image with section line (profile#1) over the wrinkles, (c) section line over the wrinkles of graphene.
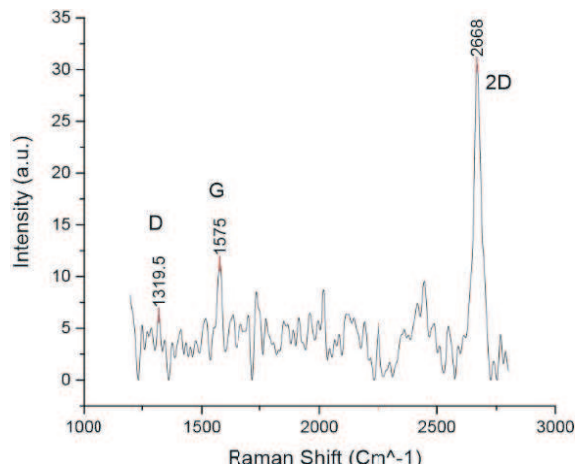
Figure 5. Raman Spectroscopy of monolayer graphene sheet transferred on glass substrate.
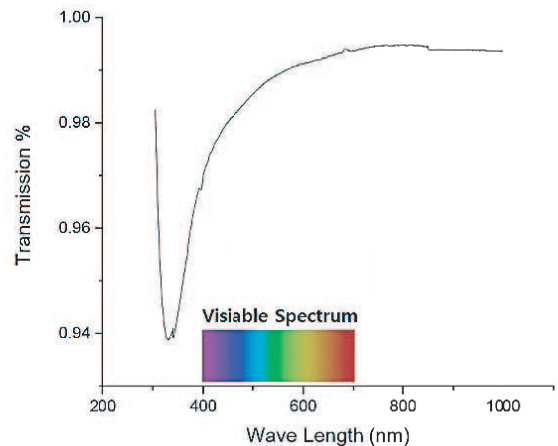
Figure 6. Transmission of graphene sample measured by spectrophotometer.
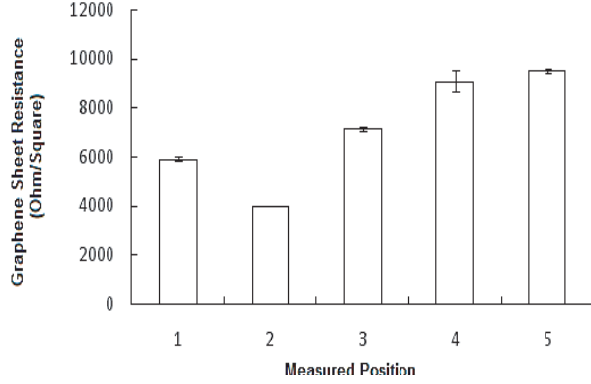
Figure 7. Graphene sheet resistivity at different measured positions.
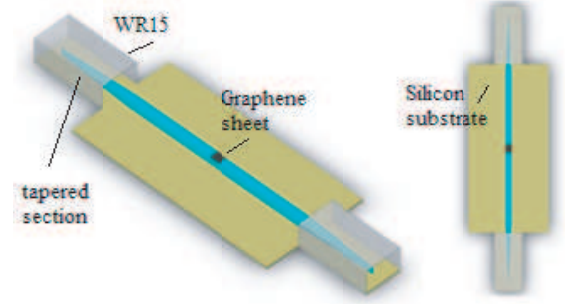
Figure 8. Schematic drawing of DIG Graphene-based frequency multiplier with 1 mm Graphene sheet on top of the DIG.

The graphene sheet resistance is not constant at all directions of the prepared graphene sheet. Fig. 7 shows values of sheet resistance between 4 and $10 \, \mathrm{k\Omega}$/square areas. This may be due to wrinkles in the graphene sheet as shown in the AFM images.

4. FREQUENCY MULTIPLIER

Frequency multiplication is a common approach for signal generation in variety of communication systems at different frequency ranges. Usually this process is realized by modulating a low frequency signal with a nonlinear device (diode or FET transistor) to generate harmonic signals at higher frequencies, and the desired frequency signal can be extracted by applying the required filter to output frequencies. Frequency multipliers based on conventional semiconductors offer acceptable conversion efficiency for the second order harmonics. However, they offer low conversion efficiency for higher multiplication orders. In our proposed design, the efficiency of higher order harmonics (7th harmonic) is higher than that proposed in [16] in addition to maintaining a satisfactory conversion efficiency for second harmonic.

A schematic diagram of the proposed design of the multiplier using DIG technology platform is shown in Fig. 8. The cross-section of the dielectric image waveguide is $800 \, \mathrm{\mu m}$ in width and $500 \, \mathrm{\mu m}$ height. The DIG can support fundamental mode at $55 \, \mathrm{GHz}$. The fabrication of the DIG includes a one mask process using high resistivity silicon wafers [8]. The process is compatible with standard IC fabrication processes and suitable for mass production which makes it very attractive to many industries. The slab is placed on top of a $130 \, \mathrm{\mu m}$ substrate connected at its two terminal ports. The input and output ports are coupled to the guide using two tapered sections and excited with the conventional WR15 rectangular metallic waveguide at input terminal of the excited wave and a WR10 from the output port. A few layer graphene with length $500 \, \mathrm{\mu m}$ is placed on top of the silicon slab to maintain the nonlinear activity.

Modeling of the graphene-based DIG multiplier is performed using Lumerical software. The output spectrum is shown in Fig. 9. The power of the input signal at $55 \, \mathrm{GHz}$ was assumed to be $10 \, \mathrm{dBm}$. The

Table 1. Harmonics conversion efficiency of the Graphene-based DIG multiplier.

Harmonic Order	Conversion Efficiency
2nd	$-23 \, \mathrm{dB}$
3rd	$-34 \, \mathrm{dB}$
4th	$-61.31 \, \mathrm{dB}$
5th	$-78 \, \mathrm{dB}$

simulated field-spectrum diagram shows the field intensity of signal at output port. Field components at higher harmonics are shown with reasonable strength up to the 5th order harmonic. The conversion frequency of the DIG multiplier is calculated as the ratio of power of the harmonics at the output port to the power of the input signal [25]. In Table 1 a frequency conversion efficiency is calculated for each harmonic field. The simulated results show -23 dB conversion efficiency for the second harmonic which is relatively higher than the designs in [15, 16]. Fig. 10 shows the scattering parameters of the design.
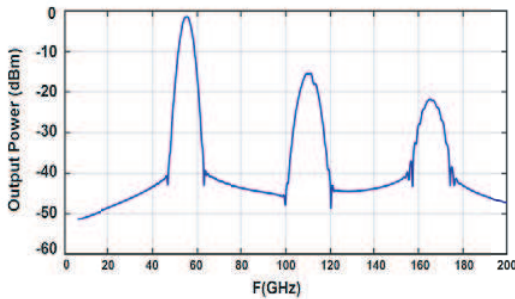
Figure 9. Spectrum of the output fields for DIG-based Graphene frequency multiplier.
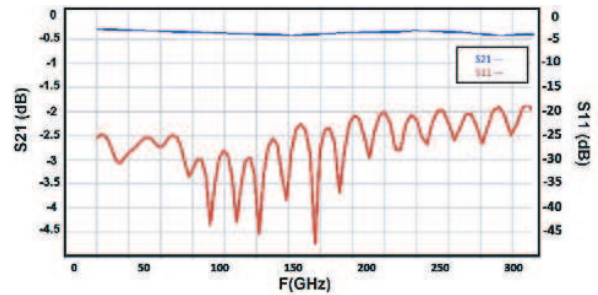
Figure 10. S-Parameters of DIG Graphene multiplier.

5. FREQUENCY MIXER DESIGN

A communication system receiver cannot be built without the aid of a frequency mixer device. Frequency mixers use nonlinear devices to perform up or down conversion of proposed input frequencies by shifting them from one frequency range to another. One example is converting the RF signal at the receiver to an intermediate signal by mixing with a local oscillator.

The proposed mixer design based on DIG technology platform using graphene as the nonlinear medium is shown in Fig. 11. The small footprint of the 2D material can propose a small receiver design with a broadband operation.

The design is based on DIG platform on a 130 μm substrate connected with two input terminal ports with two taper sections for coupling with standard WR15 and WR12 rectangular metallic waveguides excited by sources at 55 GHz and 80 GHz, respectively, combined by a DIG curved combiner and connected to a WR10 waveguide at the output port. A few layer graphene of length 500 μm is deposited on the silicon slab after the combiner stage to maintain the nonlinear activity needed for mixing the two signals.
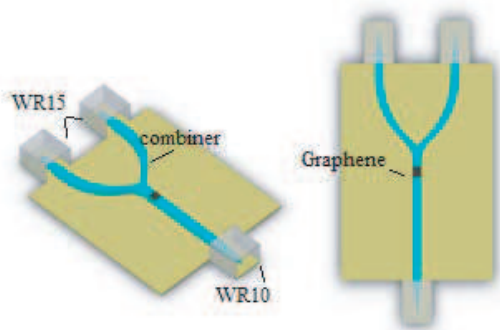
Figure 11. DIG-Graphene Mixer Design with 1 mm Graphene on top and excitation at 55 GHz and 75 GHz.
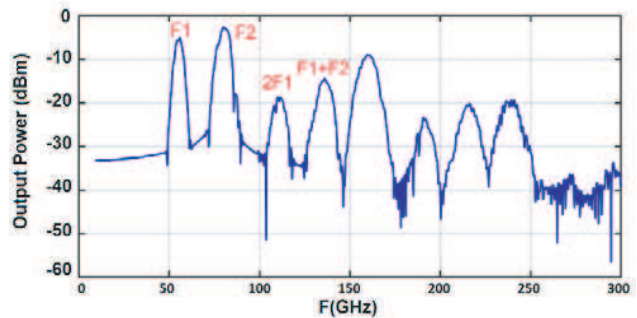
Figure 12. Mixer's Output Spectrum with 55 GHz and 75 GHz excitation signals for 1 mm Graphene sheet on DIG surface.

In Fig. 12 the frequency spectrum of the output field components is shown; the results show a very strong mixing component at the summation frequency in addition to convenient harmonics of the input signals. A conversion efficiency of the output mixed frequencies is -28 dB as shown in Fig. 12 and Table 2. This conversion efficiency is good compared to mixers in [19].

Table 2. Mixer conversion efficiency.

Order	Conversion Efficiency
Summation ($f_1 + f_2$)	-28.6 dB

6. CONCLUSION

An efficient low-cost and broadband frequency multiplier and frequency mixer devices were presented. The frequency multiplier and mixer utilized dielectric image waveguide and were based on nonlinear properties of graphene material at millimeter wave band. The simulated results showed a significantly high conversion efficiency about -23 and -28 dB for the frequency multiplier and frequency mixers, respectively which are higher than ordinary devices. The linear properties of Graphene were experimentally measured and characterized. The nonlinear properties were simulated using Lumerical Software.

ACKNOWLEDGMENT

REFERENCES

1. Bontu, C. S., D. D. Falconer, and L. Strawczynski, "Simple equalization scheme for high rate FSK data transmission in the millimeter wave frequency band," *Sixth IEEE International Symposium on Personal, Indoor and Mobile Radio Communications, 1995, PIMRC'95, Wireless: Merging onto the Information Superhighway*, Vol. 1, IEEE, 1995.
2. Bontu, C. S., D. D. Falconer, and L. Strawczynski, "Feasibility evaluation of high rate FSK data transmission and equalization for millimeter wave indoor radio," *1996 5th IEEE International Conference on Universal Personal Communications, 1996, Record*, Vol. 2, IEEE, 1996.
3. Wei, X., et al., "A wide band millimeter-wave substrate integrated coaxial line (SICL) for high speed data transmission," *2015 Asia-Pacific Microwave Conference (APMC)*, Vol. 3, IEEE, 2015.
4. Kemp, M. C., A. Glauser, and C, Baker, "Recent developments in people screening using terahertz technology: Seeing the world through terahertz eyes," *Defense and Security Symposium*, International Society for Optics and Photonics, 2006.
5. Vaseashta, A., "New THz technologies and applications in applications in support of safety and security," *THz and Security Applications*, 277–292, Springer, Netherlands, 2014.
6. Cooper, K. B., et al., "Penetrating 3-D imaging at 4-and 25-m range using a submillimeter-wave radar," *IEEE Transactions on Microwave Theory and Techniques*, Vol. 56, No. 12, 2771–2778, 2008.
7. Fakharzadeh, M., M. Nezhad-Ahmadi, B. Biglarbegian, J. Ahmadi-Shokouh, and S. Safavi-Naeini, "CMOS phased array transceiver technology for 60 GHz wireless applications," *IEEE Trans. on Antennas and Propagation*, Vol. 58, No. 4, 1093–1104, Apr. 2010.
8. Basha, M. A., et al., "Novel D-band Si-based integrated platform for millimeter wave," *2014 44th European Microwave Conference (EuMC)*, IEEE, 2014.
9. Basha, M. A., A. Samir, and R. H. Zaghloul, "Evolution of DIG integrated platform for millimeter-wave applications," *2015 IEEE Radio and Wireless Symposium (RWS)*, IEEE, 2015.
10. Glazov, M. M. and S. D. Ganichev, "High frequency electric field induced nonlinear effects in graphene," *Physics Reports*, Vol. 535, No. 3, 101–138, 2014.

11. Mikhailov, S. A., "Non-linear graphene optics for terahertz applications," *Microelectronics J.*, Vol. 40, Nos. 4–5, 712–715, 2009.

12. Ishikawa, K. L., "Nonlinear optical response of graphene in time domain," *Phys. Rev. B*, Vol. 82, No. 20, 201402, Nov. 2010.

13. Hadarig, A. I., et al., "Experimental analysis of the high-order harmonic components generation in few-layer graphene," *Applied Physics A*, Vol. 118, No. 1, 83–89, 2015.

14. Amir, F., C. Mitchell, and M. Missous, "Development of advanced Gunn diodes and Schottky multipliers for high power THz sources," *2010 8th International Conference on Advanced Semiconductor Devices & Microsystems (ASDAM)*, IEEE, 2010.

15. Ward, J., et al., "Capability of THz sources based on Schottky diode frequency multiplier chains," *2004 IEEE MTT-S International Microwave Symposium Digest*, Vol. 3, IEEE, 2004.

16. Feng, Z. H., et al., "High-frequency multiplier based on GaN planar Schottky barrier diodes," *2016 IEEE MTT-S International Microwave Workshop Series on Advanced Materials and Processes for RF and THz Applications (IMWS-AMP)*, IEEE, 2016.

17. Hanson, G. W., "Dyadic Green's functions and guided surface waves for a surface conductivity model of graphene," *Journal of Applied Physics*, Vol. 103, No. 6, 064302, 2008.

18. Niu, J., M. Luo, and Q. H. Liu, "Full-wave nonlinear optical analyses of graphene-based optoelectronic devices," *2015 USNC-URSI Radio Science Meeting (Joint with AP-S Symposium)*, IEEE, 2015.

19. Hotopan, G. R., S. Ver-Hoeye, C. Vazquez-Antuna, R. Camblor-Diaz, M. Fernandez-Garcia, F. Las Heras Andres, P. Alvarez, and R. Menéndez, "Millimeter wave microstrip mixer based on graphene," *Progress In Electromagnetics Research*, Vol. 118, 57–69, 2011.

20. Yang, K., S. Arezoomandan, and B. Sensale-Rodriguez, "The linear and nonlinear THz properties of graphene," *International Journal of Terahertz Science and Technology*, Vol. 6, No. 4, 223–233, 2013.

21. Hendry, E., P. J. Hale, J. Moger, et al., "Coherent nonlinear optical response of graphene," *Phys. Rev. Lett.*, Vol. 105, 097401, 2010.

22. Graphenea LTD, "MikeletegiPasealekua," 83, 20009 Donostia, Gipuzkoa, Spain.

23. Zhao, W., M. Fang, F. Wu, H. Wu, L. Wang, and G. Chen, "Preparation of graphene by exfoliation of graphite using wet ball milling," *J. Mater. Chem.*, Vol. 20, No. 28, 5817, 2010.

24. Takatoshi, Y., K. Jaeho, I. Masatou, and H. Masataka, "Low-temperature graphene synthesis using microwave plasma CVD," *J. Phys. D. Appl. Phys.*, Vol. 46, No. 6, 63001, 2013.

25. Falcão-Filho, E. L., et al., "Analytic scaling analysis of high harmonic generation conversion efficiency," *Optics Express*, Vol. 17, No. 13, 11217–11229, 2009.